Local Structure Refinement of Disordered Material Models: Ion Pairing and Structure in YCl_3 Aqueous Solutions

D. T. Bowron*,† and S. Diaz-Moreno‡

ISIS Facility, Rutherford Appleton Laboratory, Chilton, Didcot, OX11 0QX, U.K., and Diamond Light Source Ltd., Harwell Science and Innovation Campus, Diamond House, Chilton, Didcot, Oxfordshire, OX11 0DE, U.K.

Received: June 8, 2007

Hydrogen/deuterium isotopic neutron diffraction techniques have been used to investigate the structure of a 1 *m* aqueous solution of YCl_3 at room temperature. Empirical potential structure refinement (EPSR) has been used to build a three-dimensional model of the solution structure that is consistent with the bulk solvent correlations strongly probed by the neutron scattering technique. Optimization of the local structural environment of the Y^{3+} ion sites within the model has been performed through calculations of the yttrium K-edge, extended X-ray absorption fine structure (EXAFS) spectrum of the solution, and detailed information has been extracted on the structure of the ion hydration shell and the extent of inner-sphere ion pairing within the solution. The results demonstrate the significant potential of this hybrid data analysis approach to circumvent the limitations of the individual experimental methods, to refine atomic potential models, and to produce accurate, quantitative structural models of the local environment of dilute atomic species within tightly constrained bulk network structures.

Introduction

The experimental investigation of ion hydration structures is an important component of modern physical chemistry. The results of such studies have wide-ranging implications in numerous associated areas of research such as in understanding the stabilization or destabilization of proteins in solution[1] or the transport of minerals by geophysical mechanisms.[2] Despite the fundamental importance of aqueous electrolytes, structural interest has tended to be focused on one or the other of two primary factors, namely, (i) the geometric form of the immediate hydration shell of an ion or (ii) the impact that the presence of ions has upon the structure of the bulk solvent medium. Perhaps somewhat surprisingly, for many ions a comprehensive description of the entire salt plus solvent system is still lacking, and as a result a degree of controversy often remains regarding one or both of the above-mentioned issues. Here we address the particular case of the hydration of the yttrium III cation (Y^{3+}) and use the study to demonstrate a widely applicable approach that can give the required comprehensive insight into the structural nature of ions in disordered media. The technique is based on a combination of neutron scattering and X-ray absorption spectroscopy and combines their markedly different structural sensitivities through a reverse modeling technique.[3] This approach balances bulk and local structure information on the system, and the resulting model allows us to determine, in a manner wholly consistent with the available experimental data, both the geometric form of the ion hydration shell and the impact this has upon the overall solvent structure. Furthermore, this method provides a means by which it is possible to make a quantitative estimate of the extent of ion pairing within the solution and consequently to address this long-standing but important experimental challenge.

Recently the hydration of Y^{3+} has drawn considerable experimental and theoretical investigation,[4−6] in particular targeted at determining the geometric structure of its first hydration shell[4] as this is thought to be intimately related to the chemical activity of this ionic species in solution and its capacity to form inner-sphere ion complexes.[7] Detailed local structure studies based on extended X-ray absorption fine structure (EXAFS) spectroscopy and X-ray absorption near-edge structure (XANES) have concluded that the most preferable geometric form of the Y^{3+} hydration shell is for the oxygen atoms of eight water molecules to coordinate the ion via the formation of a square antiprism.[4] This result has recently been corroborated by a Car−Parrinello molecular dynamics simulation.[7] Despite an earlier report of inner-sphere complex formation in an yttrium selenate solution,[8] both the X-ray absorption spectroscopy[4,9] and X-ray diffraction experiments[5,6,10] found no conclusive evidence for direct ion-pair interactions in the more widely studied yttrium halide systems, though it is worth pointing out that the contribution from such species to the experimental signals is likely to be very weak given the intrinsic structural disorder in this liquid-state system.

Experimental Section

At the core of this experimental study are a series of three neutron scattering measurements performed on solutions of YCl_3 in H_2O, D_2O, and HDO, at a concentration of 1 Y^{3+} ion to 55.5 water molecules at a temperature of 298 K. The result of each of these measurements is an interference differential cross section or total structure factor, $F(Q)$, defined as

$$F(Q) = \sum_{\alpha \le \beta} (2 - \delta_{\alpha\beta}) c_\alpha c_\beta b_\alpha b_\beta [S_{\alpha\beta}(Q) - 1] \qquad (1)$$

c_α, c_β and b_α, b_β are the atomic fractions and neutron scattering lengths of each type of atom in the sample and weight the contributions from each of the partial structure factors

* Corresponding author. E-mail: D.T.Bowron@rl.ac.uk.
† Rutherford Appleton Laboratory.
‡ Diamond Light Source Ltd.

10.1021/jp0744580 CCC: $37.00
Published on Web 09/13/2007

TABLE 1: Atomic Fractions and Neutron Scattering Lengths for the Constituents of the 1 *m* Aqueous Solutions of YCl_3

atom type	concn	scattering length (fm)
H	0.6491	−3.74
D		6.67
H/D		1.47
O	0.3246	5.80
Y	0.0058	7.75
Cl	0.0175	9.58
H(HNO_3)	0.0006	−3.74
N(HNO_3)	0.0006	9.36
O(HNO_3)	0.0018	5.80

$[S_{\alpha\beta}(Q) - 1]$ to the measured total structure factor. Q is the magnitude of the momentum transfer vector in the scattering process for neutrons of incident wavelength λ and scattering angle 2θ; it is defined as

$$Q = \frac{4\pi}{\lambda} \sin\theta \tag{2}$$

$\delta_{\alpha\beta}$ is the Kronecker δ function to avoid double counting the interactions between atoms of the same type. The concentrations and neutron scattering lengths used in this study are given in Table 1.

The partial structure factors are related to the more intuitive partial pair distribution functions $g_{\alpha\beta}(r)$ by a Fourier transform weighted by the atomic density of the system, ρ, and shown in eq 3.

$$g_{\alpha\beta}(r) - 1 = \frac{1}{(2\pi)^3\rho}\int_0^\infty 4\pi Q^2[S_{\alpha\beta}(Q) - 1]\frac{\sin Qr}{Qr}\,\mathrm{d}Q \tag{3}$$

These functions allow us to directly picture the structure of the system via the relative probability of finding atoms of type β around type α, as a function of their separation distance, r.

Though it is experimentally very challenging to directly obtain all the partial structure factors that are required to characterize a multicomponent system, by combining the measurements on the three isotopically distinct samples using second-order difference techniques, the neutron scattering experiment can directly probe the detailed structure of the solvent water from the viewpoint of the water hydrogen atoms.[11] Though not directly probing the ion−water correlations the technique does also provide useful information on the accommodation of the ionic species within the solution in terms of some complex cross-correlations reflecting the pairwise interactions between the isotopically substituted and nonsubstituted atomic species in the solution. It is worth noting that due to the relative concentrations of the ionic components in the mixture, the structural correlations not involving water molecules make a considerably weaker contribution to the measured differential scattering cross sections.

The neutron scattering experiments were performed on the SANDALS diffractometer at the ISIS pulsed spallation neutron source, U.K. The samples were contained in $Ti_{0.68}Zr_{0.32}$ alloy flat plate cells of wall thickness of 1.1 mm and of internal dimensions of 1 mm × 35 mm × 35 mm. By virtue of the alloy composition, the sample cell makes no contribution to the coherent scattering signal that contains the structural information from the sample. The data were corrected for absorption and multiple scattering and were normalized to the scattering of a known vanadium standard using the methods outlined in the ATLAS package[12] and finally reduced to interference differential cross sections, $F(Q)$, by the methods outlined in Soper and Luzar.[13] To prevent the formation of hydroxide complexes within the solutions, the samples were acidified to pH 1 by the addition of a structurally insignificant quantity of nitric acid. The atomic densities of the solutions were determined to be 0.1 atoms·Å^{-3} with an Anton Paar DMA-4100 density meter.

TABLE 2: Lennard-Jones and Charge Parameters Used in the Simulation of YCl_3 Aqueous Solutions[a]

atom	ϵ [kJ/mol]	σ [Å]	q [e]
O_{water}	0.6500	3.166	−0.8476
H_{water}	0.0000	0.000	+0.4238
Y (model 1)	0.1250	3.250	+3.0000
Y (model 2)	0.1250	3.100	+3.0000
Cl	0.4190	4.380	−1.0000
H_{H+}	0.0075	0.000	−1.0000
N_{NO3-}	0.7000	3.250	0.0000
O_{NO3-}	0.8000	0.296	−0.3333

[a] These are combined using the Lorenz−Berthelot mixing rules: $\sigma_{\alpha\beta} = 1/2[\sigma_\alpha + \sigma_\beta]$, $\epsilon_{\alpha\beta} = [\epsilon_\alpha\epsilon_\beta]^{1/2}$.

Data Modeling

To maximize the structural information that could be extracted from the experimental data the technique of empirical potential structure refinement (EPSR)[14,15] has been used to build a three-dimensional model consistent with the neutron scattering data. The technique first performs a standard Monte Carlo simulation of the system using known information regarding intramolecular structure, the bulk atomic density, and a set of Lennard-Jones atomic reference potentials, see Table 2. For this study, the model consists of a cubic box of side length 32.46 Å containing 20 Y^{3+} cations, 60 Cl^- anions, 1110 water molecules, plus 2 H^+ ions and 2 NO_3^- ions to account for the small amount of nitric acid used to acidify the solutions to pH 1. After this simulation equilibrates, structural difference functions are calculated between the model and the functions derived from the scattering data. These functions are then used to generate a set of empirical potential perturbation functions that iteratively drive the simulation into agreement with the scattering data.[15] Once agreement between model and data is reached and the simulation ceases to evolve, the model is deemed an acceptable representation of the structure. The simulation is then allowed to proceed under the refined potential parameters, and structural information is derived in the form of ensemble averages. These average structural functions can then be interrogated to provide detailed insight into the atomic correlations. Due to the fact that the sensitivity of the neutron scattering experiment is primarily to the bulk solution structure, and furthermore weighted toward the solvent water molecule interactions by the isotopic series, this model provides a stringent set of constraints on the environment into which the ion hydration structures must be incorporated.

Results

Water Structure. Figure 1 shows the experimentally measured $F(Q)$ for the three isotopic solutions and the corresponding fits and fit residuals to the data given by the EPSR model. As previously stated, the model is strongly weighted toward the bulk solvent correlations in this aqueous solution, and Figure 2 shows the partial pair distribution functions, $g(r)$, for the water hydrogen and water oxygen correlations extracted from the simulation, compared with the corresponding functions determined in similar fashion for pure water.[16]

From an examination of this figure, differences can be seen in all three of the partial distribution functions. The most significant structural changes from the pure water system are found in the solvent's O_{water}−O_{water} pair distribution function,

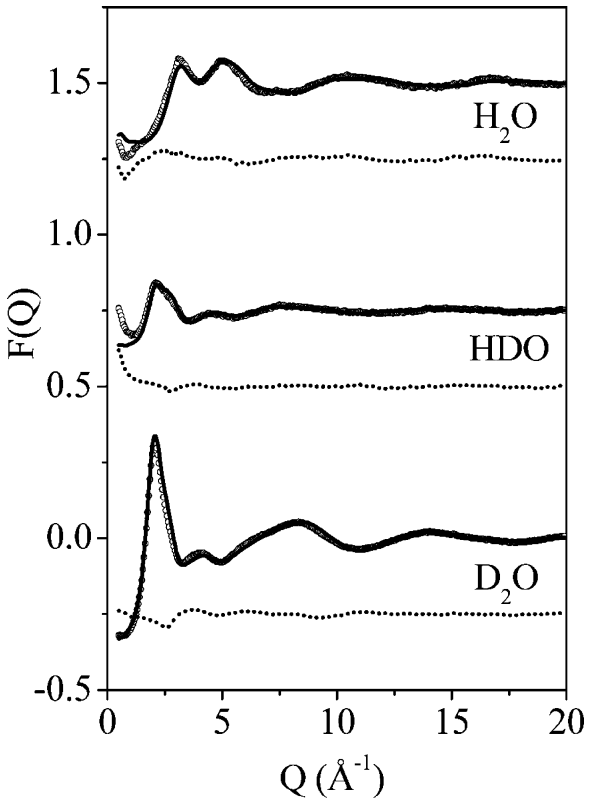

Figure 1. Interference differential cross sections, $F(Q)$, measured for 1 *m* YCl_3 in D_2O, HDO, and H_2O. The open circles correspond to the experimental data, the solid lines to the EPSR model, and the dotted lines to the fit residuals.

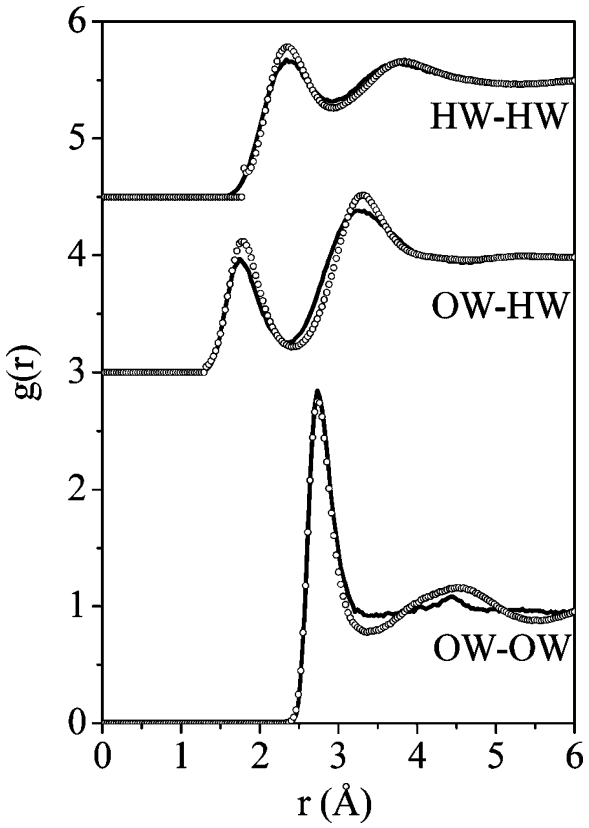

Figure 2. Intermolecular $O_{water}-O_{water}$, $O_{water}-H_{water}$, and $H_{water}-H_{water}$ pair distribution functions for a 1 *m* aqueous solution of YCl_3 at 298 K (solid line) compared with the same functions for pure water (open circles).

and these changes are most evident at the second-neighbor and greater distance range. Though the first-neighbor interactions between water molecules appear very similar to those that would be found in the pure liquid, integration of the first peak in this function, in the distance range from 2.3 to 3.3 Å, tells us that the average coordination of water oxygens atoms by other water oxygen atoms in the 1 *m* YCl_3 solution is 4.5 ± 0.1. This is slightly greater than the value of 4.3 ± 0.1 which is characteristic of liquid water and is consistent with the earlier observation that the addition of ions to water induces local structural effects analogous to the application of pressure to a pure water system.[17] The changes beyond 3.3 Å are also found to be considerably greater than those recently observed in a neutron scattering study of water structure perturbed by monovalent ions.[18] Interestingly, the areas of the first peaks of the $O_{water}-H_{water}$ and $H_{water}-H_{water}$ pair distribution functions correspond to 1.7 ± 0.1 hydrogen neighbors around each water oxygen atom in the distance range between 1.4 and 2.5 Å, and 5.2 ± 0.1 hydrogen atoms in the distance range from 1.5 to 3.0 Å around each water hydrogen site. Whereas the $O_{water}-O_{water}$ function showed evidence of liquid compression through a slight increase in the local coordination number, these hydrogen-focused correlations suggest a compensating reduction in local atomic density as the corresponding integrals for the pure liquid in the same distance ranges are 2.0 ± 0.1 for $O_{water}-H_{water}$ and 5.6 ± 0.1 for $H_{water}-H_{water}$. The move to longer correlation distances for the H_{water} interactions can also be seen in the shift in intensity from the first peaks in the $O_{water}-H_{water}$ and $H_{water}-H_{water}$ pair distribution functions to the region around 3.0 Å.

Clearly, the system thus displays an interesting topological change from the pure liquid that brings the oxygen sites closer together while moving the hydrogen sites further apart. How this is accommodated can be seen in Figure 3, which shows the spatial density functions[19] for the first- and second-neighbor shells of water oxygen atoms around any arbitrarily selected water molecule in the aqueous solution, compared with the corresponding functions for pure water. The comparison shows that the most significant change in the first-neighbor distribution occurs in the spreading of the isosurface region in the H−O−H plane, and corresponding to neighboring water molecules coordinated to the lone-pair region of the central water molecule in the ion containing solution. The second-neighbor spatial distribution can also be seen to be markedly changed by the presence of the ions in the solution, with an increased localization of the water molecules coordinating the region influenced by the hydrogen bonds donated from the central molecule, and an expansion out of the H−O−H plane, of the central molecule's lone-pair-mediated second-neighbor distribution.

Ion Hydration. The EPSR fits and residuals shown in Figure 1 tell us that the structural model for the YCl_3 solution is reasonable from the perspective of the solvent as these structural correlations dominate the measured neutron total structure factors. However, consideration of the weighting factors in eq 1 immediately highlights that the structural correlations involving the ionic species are relatively weakly represented in their contribution to the data used to generate the model. The challenge is therefore to determine whether this model also satisfactorily incorporates the local structural correlations involving the ionic species and, in this case specifically, the structural accommodation of the Y^{3+} cation. To evaluate the quality of the model for reproducing the hydration structure of this ion it is necessary to benchmark the evaluated structure against a sensitive measure of the ion's local environment. As shown in the many previous experimental studies of this system,[4,9] an ideal probe for this purpose is X-ray absorption

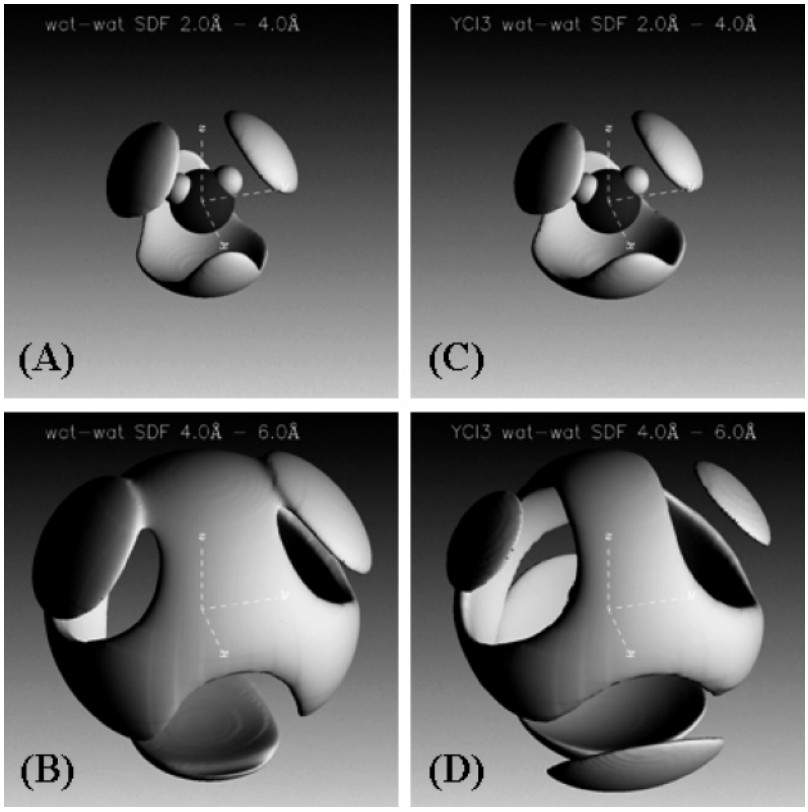

Figure 3. Pure water (A and B) and 1 *m* YCl_3 solution (C and D) water−water spatial density functions showing the 30% most probable isosurface for finding a water oxygen atom around an arbitrarily selected water molecule within the system. Panels A and C show the first-neighbor spatial distribution in the distance range from 2 to 4 Å around a water molecule at the origin, and panels B and D show the second-neighbor spatial distribution in the distance range from 4 to 6 Å from the origin.

spectroscopy. Here we report an extension of the EPSR method that provides an ability to calculate EXAFS spectra for specific components within the simulation box.

Several advanced computer codes now exist that allow accurate calculation of EXAFS spectra,[20−23] and for each, the fundamental requirement for generating the necessary spectral functions is simply a set of atomic coordinates and the corresponding types for atoms within the local vicinity of a photoabsorbing atom site within the system of interest. The extraction of such information from a three-dimensional computer model is a trivial step, and consequently, it is possible to use this information to generate a series of EXAFS spectra for each photoabsorbing site within a model and to ensemble average the result. For this analysis, the local atomic environments for the Y^{3+} sites within the EPSR model have been extracted out to a radial distance of 6 Å and used as the input for the full multiple scattering X-absorption calculation code, FEFF 8,[20] that calculates the scattering potentials, photoelectron scattering paths, and spectral contributions for each site in turn. The resulting EXAFS spectra were then ensemble averaged in identical fashion to the normally derived structural functions from a classical simulation, and the result was compared with the appropriate experimental data, here taken from ref 4. A particular advantage of this analysis route is that it avoids the well-known difficulties for refining EXAFS data obtained from highly disordered systems,[24] as no approximations are required for peak shapes or Debye−Waller factors. The disorder in the system is intrinsically captured by the three-dimensional structural model, and the only free parameter in the calculation chain is the magnitude of the offset to the energy scale zero point, ΔE_0, which for this system was found to be optimal for a fixed value of 4 eV. To appropriately capture the disorder that is reflected in the model, it proved necessary to average the EXAFS signals calculated for several hundred ion sites.

Though not new, the approach of combining EXAFS analysis codes with classical Monte Carlo or molecular dynamics simulation methods is a rapidly developing field[25] and is strongly driven by the increasing capabilities of modern computer systems. The use of reverse techniques that build structures that are consistent with experimental EXAFS data constraints is somewhat more limited, though recently techniques have been developed that use the spectra to direct the evolution of local structural models,[26,27] though without the use of atomic potential models. In contrast to these two established approaches, the technique adopted here is a hybrid that makes use of an atomic potential based directed modeling procedure, EPSR, to first build a global three-dimensional structure that is consistent with neutron or X-ray diffraction data, and which is then followed by the use of the classical analysis methods[25] to generate predictive comparisons of the local structure of the photoabsorbing atom sites. This combined methodology allows us to establish whether the local environments that exist for these sites within the global model can be considered a reasonable representation for the system of interest and also to explore details of how subtle changes in the atomic interaction potentials can effect the local structural environment of photoactive species at a level that is far beyond the sensitivity limit of the diffraction techniques.

Figure 4 shows the EXAFS data for the Y^{3+} cation at 1 *m* concentration[4] and corresponding theoretical spectra calculated from two EPSR models, both of which were found to reproduce the neutron diffraction data equally well with no observable difference to the results shown in Figure 1. Model 1 represents the result of the calculation where the Lennard-Jones reference

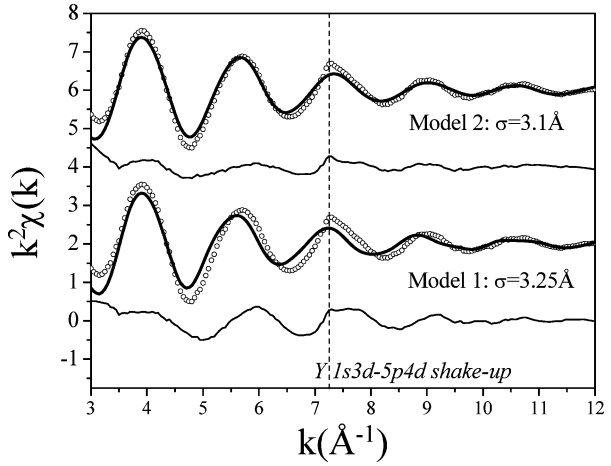

Figure 4. EXAFS data (open circles) for 1 *m* Y^{3+} in aqueous solution (ref 4) and theoretical calculations (thick solid lines) and residuals (thin solid lines), corresponding to two EPSR models. Model 1 assigns a Lennard-Jones σ to the Y^{3+} ion of 3.25 Å that results in an average $Y^{3+}-O_{water}$ distance of 2.39 Å. Model 2 assigns a Lennard-Jones σ to the Y^{3+} ion of 3.10 Å that results in an average $Y^{3+}-O_{water}$ distance of 2.33 Å.

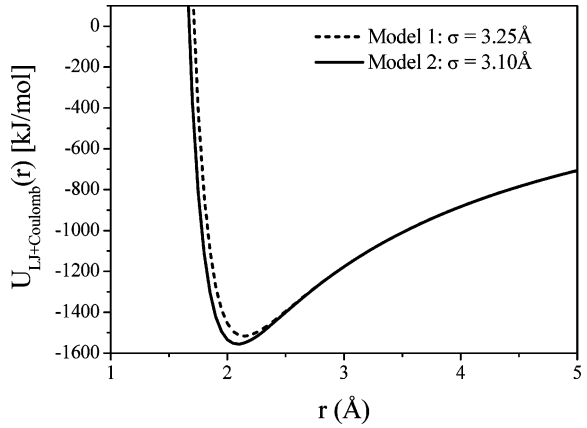

Figure 5. Comparison of the $Y^{3+}-O_{water}$ interaction potentials used to generate the two local structure models used in the calculation of the EXAFS spectra.

potential for the Y^{3+} cation was chosen to give an average $Y^{3+}-O_{water}$ distance of 2.39 Å, by adopting a value of the Lennard-Jones σ of 3.25 Å. This distance is midway in the range reported for the $Y^{3+}-O_{water}$ interaction in the literature, 2.33−2.46 Å.[4−10] On inspection the calculated EXAFS signal can clearly be seen to be out of phase with the experimentally measured function. Variation of ΔE_0 within the EXAFS theory demonstrated that this mismatch could not be simply corrected. In contrast, model 2 was performed using a value of the Y^{3+} Lennard-Jones σ of 3.1 Å. This produced a model in which the average value of the $Y^{3+}-O_{water}$ distance is 2.33 Å, consistent with the spectroscopic[4,9] and modern anomalous X-ray scattering[6] determinations. On comparison with the experimental data model 2 results in an estimation of the EXAFS signal from the Y^{3+} ion that is comparable in quality with a conventional direct analysis.[4] The spectral feature at $\approx$7.2 $Å^{-1}$ arises from the simultaneous excitation of an Y^{3+} 3d electron to a 4d level with the principle X-ray excitation of the Y^{3+} 1s electron to a 5p level.[28] As multielectron excitations are not included in the basic FEFF calculation of the EXAFS signal, this feature is absent from the model.

Figure 5 demonstrates the sensitivity of the X-ray absorption data to the details of the local atomic interaction potentials through a comparison of the $Y^{3+}-O_{water}$ potential that results from the two choices of Lennard-Jones σ. The figure effectively illustrates how EXAFS data provide us with a powerful means by which it is be possible to tune the models used for the atomic reference potential in classical simulation studies. Such fine-tuning of the aqueous electrolyte models would not be possible using the diffraction information alone since, as previously pointed out, the contribution of the local ion structure to the experimental signal is generally only a small fraction of the total scattering signal from these solutions.

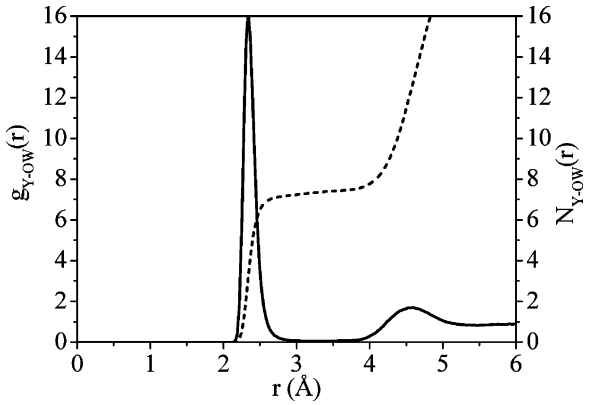

Figure 6. $Y^{3+}-O_{water}$ pair distribution function (solid line) and running coordination number $N(r)$ (dashed line) for 1 *m* YCl_3 in aqueous solution from the EXAFS spectroscopy optimized EPSR model.

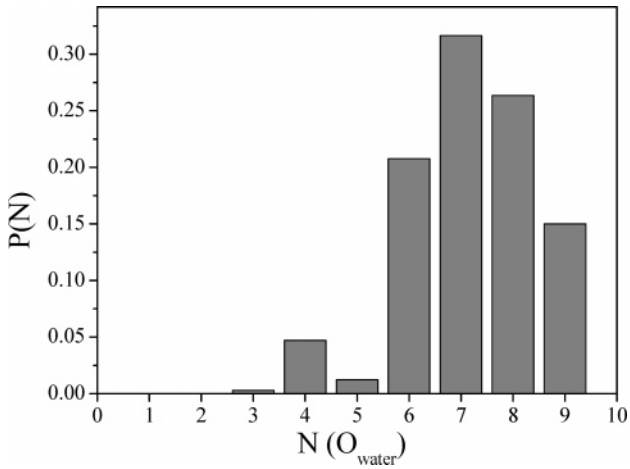

Figure 7. $Y^{3+}-O_{water}$ hydration histogram showing the relative probabilities for finding a water molecule within the first hydration shell, i.e., for the water oxygen atom to be within the distance range between 2.0 and 3.0 Å of the cation.

Model 2 is a comprehensive structural representation of the solution that captures the key elements of the bulk structure from the viewpoint of the neutron scattering experiment and simultaneously the local structure of the Y^{3+} sites via the reproduction of the EXAFS spectrum. Interrogation of this three-dimensional model can now let us further investigate the system beyond the previously discussed ion-induced structural perturbation to the water network. In particular it is now possible to study with confidence the local hydration geometry of the Y^{3+} cation and the extent of inner-sphere ion complexation in this system.

Figure 6 shows the $Y^{3+}-O_{water}$ pair distribution function and the running coordination number. It can be seen that, on average, the first hydration shell of the cation contains 7.4 $\pm$ 0.5 water molecules in the distance range between 2.1 and 3.3 Å. The hydration number histogram analysis of the model, Figure 7, shows that this mean value is derived from a distribution in which coordination by seven or eight water molecules is the

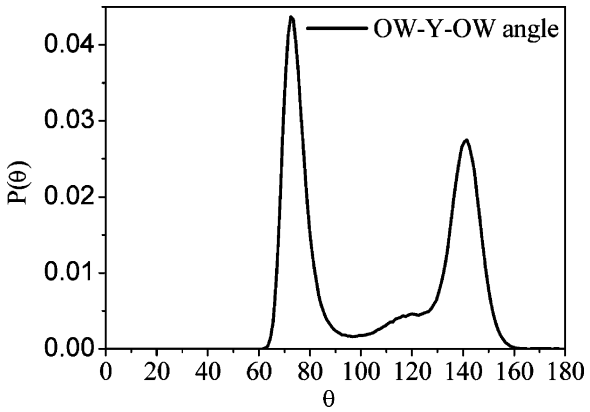

Figure 8. $O_{water}-Y^{3+}-O_{water}$ bond angle distribution illustrating the high probability of finding 70° and 140° configurations consistent with the previously assigned preference for a local hydration shell of square antiprism form.

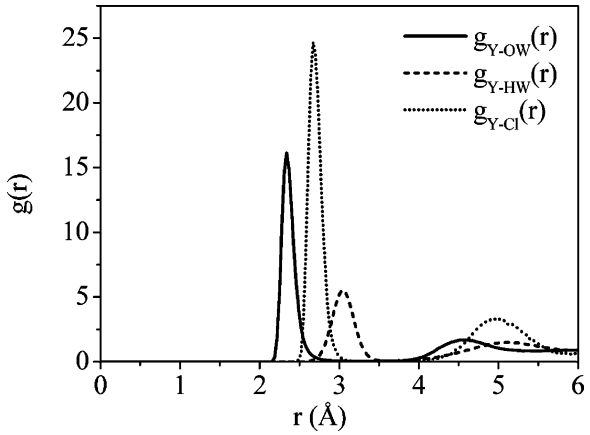

Figure 9. $Y^{3+}-O_{water}$ (solid line), $Y^{3+}-H_{water}$ (dashed line), and $Y^{3+}-Cl^-$ (dotted line) pair distribution functions evaluated from the EXAFS spectroscopy optimized EPSR model and highlighting the presence of inner-sphere ion pairing between Y^{3+} and Cl^- in the 1 *m* aqueous solution of YCl_3.

most likely but that also six or 9-fold coordination by water is also a reasonably common occurrence. The corresponding $O_{water}-Y^{3+}-O_{water}$ bond angle distribution, Figure 8, is found to be very similar to that reported in the recent Car−Parrinello simulation[7] and is a strongly peaked bimodal distribution picking out preferred angular configurations of 72° and 141°. This is fully consistent with the known preferred local hydration geometry of a square antiprism centered on the Y^{3+} sites.[4,7] When considered alongside the hydration number histogram, the high specificity of the angular correlation tells us that even when eight water molecules are not present in the hydration shell the local structure still appears to favor this underlying geometry.

Ion Pairing. Due to the very weak contribution that ion pairing makes to the diffraction or spectroscopic experimental signals, previous direct analyses of scattering or spectroscopy data have been unable to estimate the extent of ion pairing that takes place in this system. At the studied 1 *m* solution concentration, and assuming that each Y^{3+} cation is hydrated by eight water molecules on average, and each Cl^- anion by six water molecules,[18] a high degree of ion pairing has to be expected. The significant advantage of the computer model based analysis methodology is that these weakly weighted functions can be evaluated in a manner that is consistent with all the available constraints, atomic density, solution composition, and diffraction and spectroscopy data.

Figure 9 shows the $Y^{3+}-O_{water}$, $Y^{3+}-H_{water}$, and $Y^{3+}-Cl^-$ pair distribution functions and clearly demonstrates that in this model, direct inner-sphere ion pairing is seen to occur. Integration of the first peak in the $Y^{3+}-Cl^-$ $g(r)$ tells us that on average each Y^{3+} cation is likely to find 0.8 ± 0.2 Cl^- anions in the distance range between 2.5 and 3.5 Å, i.e., within the first water hydration shell. This result appears to explain why even when the first hydration shell of the Y^{3+} cation contains less than eight water molecules, the $O_{water}-Y^{3+}-O_{water}$ angular distribution remains relatively unperturbed. We can hypothesize that when the hydration number of the cation is <8, the distribution of the hydrating water molecules must accommodate the presence of a Cl^- anion that would occupy a similar volume of space in the first hydration shell to the water molecule is replaces.

Conclusions

This study shows the significant perturbation to the structure of water that is induced by the addition of highly charged ionic solutes. The bulk structural changes combine an effective compression of the solvent structure when viewed from the perspective of O_{water} to O_{water} correlations. Interestingly, this is accompanied by a reduction in the number of O_{water} to H_{water} and H_{water} to H_{water} interactions in the short range, a topological modification that explains the observation that the bulk atomic density of the 1 *m* YCl_3 solution at room temperature remains very similar to that of pure water, at 0.1 atoms·Å^{-3}.

The addition of spectroscopic information to the already powerful technique of diffraction data directed three-dimensional modeling has been found to bring several significant benefits and new opportunities for the application of these techniques to the study of disordered systems.

(i) The technique provides a means to enhance the reliability of bulk structural modeling for addressing questions at a local level where often the important physical and chemical interactions occur.

(ii) The exceptional sensitivity of the spectroscopic probe to dilute atomic species in bulk matrices greatly enhances the potential application of techniques in this area. Diffraction data alone would not be able to yield any information about the minor system components.

(iii) The method allows the limitations of conventional EXAFS spectroscopy analysis methods for studying disordered material systems to be circumvented by using the diffraction experiment and the bulk three-dimensional model to directly provide information on appropriate atomic distributions function forms. This removes the need for any ad hoc disorder parameters in the models.

(iv) The method reduces the number of free parameters utilized in the EXAFS analysis to one, ΔE_0, the choice of the energy offset for the spectral signals.

(v) The method allows the investigation of how atomic potential models can be improved for incorporation into independent simulations by taking advantage of the high sensitivity of the X-ray absorption probe to the short-range details of these functions.

Areas of technological science that could immediately benefit from this analysis method include the study of optically active metal centers in telecommunications glasses and the study of the chemically active sites in homogeneous and heterogeneous catalysts.

References and Notes

(1) Mahler, H. R.; Cordes, E. H. *Biological Chemistry*; Harper and Row: New York, 1971.

(2) Mavrogenes, J. A.; Berry, A. J.; Newville, M.; Sutton, S. R. *Am. Mineral.* **2002**, *87*, 1360.
(3) McGreevy, R. L. *J. Phys.: Condens. Matter* **2001**, *13*, R877.
(4) Díaz-Moreno, S.; Muñoz-Páez, A.; Chaboy, J. *J. Phys. Chem. A* **2000**, *104*, 1278.
(5) Lindqvist-Reis, P.; Lamble, K.; Pattanaik, S.; Persson, I.; Sandström, M. *J. Phys. Chem. B* **2000**, *104*, 402.
(6) Ramos, S.; Neilson, G. W.; Barnes, A. C.; Mazuelas, A. *J. Phys. Chem. B* **2001**, *105*, 2694.
(7) Ikeda, T.; Hirata, M.; Kimura, T. *J. Chem. Phys*. **2005**, *122*, 024510.
(8) Johansson, G.; Wakita, H. *Inorg. Chem*. **1985**, *24*, 3047.
(9) de Barros Marques, M. I.; Alves Marques, M.; Resina Rodrigues, J. *J. Phys.: Condens. Matter* **1992**, *4*, 7679.
(10) Matsubara, E.; Okuda, K.; Waseda, Y. *J. Phys.: Condens. Matter* **1990**, *2*, 9133.
(11) Finney, J. L.; Soper, A. K. *Chem. Soc. Rev.* **1994**, *23*, 1.
(12) Soper, A. K.; Howells, W. S.; Hannon, A. C. *ATLAS—Analysis of Time-of-Flight Diffraction Data from Liquid and Amorphous Samples*; RAL 89-046; Rutherford Appleton Laboratory: Chilton, U.K., 1989.
(13) Soper, A. K.; Luzar, A. *J. Chem. Phys.* **1997**, *97*, 1320.
(14) Soper, A. K. *Chem. Phys.* **1996**, *202*, 298.
(15) Soper, A. K. *Phys. Rev. B* **2005**, *72*, 104204.
(16) Soper, A. K. *Chem. Phys.* **2000**, *258*, 121.
(17) Leberman, R.; Soper, A. K. *Nature* **1995**, *378*, 364.
(18) Soper, A. K.; Weckström, K. *Biophys. Chem.* **2006**, *124*, 180.
(19) Svishchev, I. M; Kusalik, P. G. *J. Chem. Phys*. **1993**, *99*, 3049.
(20) Ankudinov, A. L.; Ravel, B.; Rehr, J. J.; Conradson, S. D. *Phys. Rev. B* **1998**, *58*, 7565.
(21) Filipponi, A.; Di Cicco, A.; Natoli, C. R. *Phys. Rev. B* **1995**, *52*, 15122.
(22) Filipponi, A.; Di Cicco, A. *Phys. Rev. B* **1995**, *52*, 15135.
(23) Binsted, N. *EXCURV98:CCLRC Daresbury Laboratory Computer Program*; Daresbury Laboratory: Daresbury, U.K., 1998.
(24) Filipponi, A. *J. Phys.: Condens. Matter* **2001**, *13*, R23.
(25) Ferlat, G.; Soetens, J.-C.; San Miguel, A.; Bopp, P. A. *J. Phys.: Condens. Matter* **2005**, *17*, S145.
(26) Ansell, S.; Neilson, G. W. *Biophys. Chem.* **2004**, *107*, 229.
(27) Di Cicco, A.; Trapananti, A. *J. Phys.: Condens. Matter* **2005**, *17*, S135.
(28) Chaboy, J.; Muñoz-Paez, A.; Díaz-Moreno, S. *Chem. Eur. J*. **2001**, *7*, 1102.